Binding of NAP-22, a Calmodulin-Binding Neuronal Protein, to Raft-like Domains in Model Membranes†

Tapan K. Khan,‡ Bing Yang,‡ Nancy L. Thompson,§ Shohei Maekawa,|| Richard M. Epand,⊥ and Ken Jacobson*,‡,#

Department of Cell and Developmental Biology, Department of Chemistry, and Lineberger Comprehensive Cancer Center, University of North Carolina at Chapel Hill, Chapel Hill, North Carolina 27599, Department of Biochemistry, McMaster University, Hamilton, Ontario, Canada L8N 3Z5, and Division of Bioinformation, Department of Life Science, Graduate School of Science and Technology, Kobe University, Rokkodai, Nada-ku, Kobe 657-8501, Japan

Received August 6, 2002; Revised Manuscript Received February 19, 2003

ABSTRACT: The cholesterol-binding protein NAP-22 is a major component of the detergent-insoluble low-density fraction of rat brain. In this study, we found, using fluorescence microscopy, that native NAP-22, but not a demyristoylated form, binds to cholesterol-rich raft-like domains in planar-supported monolayers and remains bound after nonionic detergent extraction. NAP-22 also protects the cholesterol-rich domains during extraction by methyl-β-cyclodextrin. The lateral mobility of this protein is much lower than that of other raft components in model membranes, suggesting that both cholesterol binding and inter-NAP-22 interactions markedly reduce its lateral diffusion. This study suggests that NAP-22 binding may be employed to image cholesterol-rich regions, such as caveolae/rafts, on the plasma membrane of cells, and preliminary efforts in that direction are presented.

In the past decade, evidence has been accumulating for the existence of cholesterol- and sphingolipid-rich membrane microdomains (*1*, *2*) that may have important functional consequences. Controversy arises from the fact that rafts are defined biochemically with no unambiguous structural correlate at this juncture (*3*, *4*). The simplest version of the raft hypothesis postulates the coexistence of cholesterol-rich, liquid-ordered (l_o) and cholesterol-poor, liquid-disordered (l_d) domains in the membrane (*2*, *3*, *5*, *6*). In the liquid-ordered raft phase into which raft components partition, lipid acyl chains are tightly packed and ordered, although components remain laterally mobile. That such a simple view could possibly obtain in complex biomembranes which are dynamic nonequilibrium structures whose composition may vary due to membrane insertion and retrieval events has been challenged (*7*). Alternatively, it has been pointed out that "rafts" may comprise the vast majority of the plasma membrane with only a minor fraction of fluid lipid inclusions (*8*). On the other hand, caveolae/rafts may comprise a minor fraction of the membrane area with the majority of raft-resident proteins being surrounded by small lipid "shells" that are capable of coalescing into larger caveolae (*4*).

Certainly, the detection of membrane microdomains poses a formidable challenge for the membrane biologist and biophysicist. To assist in the microscopy of caveolae/rafts, one approach is to design chemical probes that bind raft constituents. For example, Waheed et al. (*9*) have explored the selective binding capability of a perfringolysin O derivative to cholesterol-rich membrane domains. The present work is another step in development of chemical tools utilizing the cholesterol-binding property of NAP-22, a neuronal protein, to study lateral heterogeneity in biomembranes.

NAP-22 is a 22 kDa acidic calmodulin-binding neuronal protein that is myristoylated (*10*, *11*). It is localized in synaptic terminals, dendritic spines, and thin nerve fibers (*12*). NAP-22 is similar in physicochemical properties to growth regulating proteins including GAP-43, B-50, neuromodulin, and MARCKS[1] (myristoylated alanine-rich C kinase substrate) (*10*). NAP-22 predominantly localizes in the Triton-insoluble low-density fraction. It binds specifically to cholesterol-containing sonicated liposomes (*11*) as well as large vesicles (*13*). A recent report shows that NAP-22 contains a significant amount of β-structure that is not sensitive to binding of the protein to membranes (*13*).

In a previous publication, we have shown that the formation of glycosphingolipid- and cholesterol-rich lipid domains can be driven solely by characteristic lipid−lipid interactions (*6*). It also has been shown that NAP-22 bound to liposomes containing dipalmitoylphosphatidylcholine (DPPC) and 40 mol % cholesterol is recovered in the detergent-insoluble

† This work was supported by NIH Grant GM41402 (K.J.), NSF Grant MCB-0130589 (N.L.T.), and Grant MT-7654 from the Canadian Institutes of Health Research (R.M.E.).

* To whom correspondence should be addressed at the Department of Cell and Developmental Biology, University of North Carolina at Chapel Hill, CB 7090, Chapel Hill, NC 27599.

‡ Department of Cell and Developmental Biology, University of North Carolina.

§ Department of Chemistry, University of North Carolina.

|| Division of Bioinformation, Department of Life Science, Graduate School of Science and Technology, Kobe University.

⊥ Department of Biochemistry, McMaster University.

Lineberger Comprehensive Cancer Center, University of North Carolina at Chapel Hill.

[1] Abbreviations: DOPC, 1,2-dioleoyl-*sn*-glycero-3-phosphocholine; Chol, cholesterol; DPPC, dipalmitoylphosphatidylcholine; DPPE, dipalmitoylphosphatidylethanolamine, SM, sphingomyelin; GM1, ovine ganglioside GM1; CTxB, cholera toxin B subunit; Rh-CTxB, rhodamine conjugated with cholera toxin B subunit; MARCKS, myristoylated alanine-rich C kinase substrate; MβCD, methyl-β-cyclodextrin.

10.1021/bi0265877 CCC: $25.00
Published on Web 04/05/2003

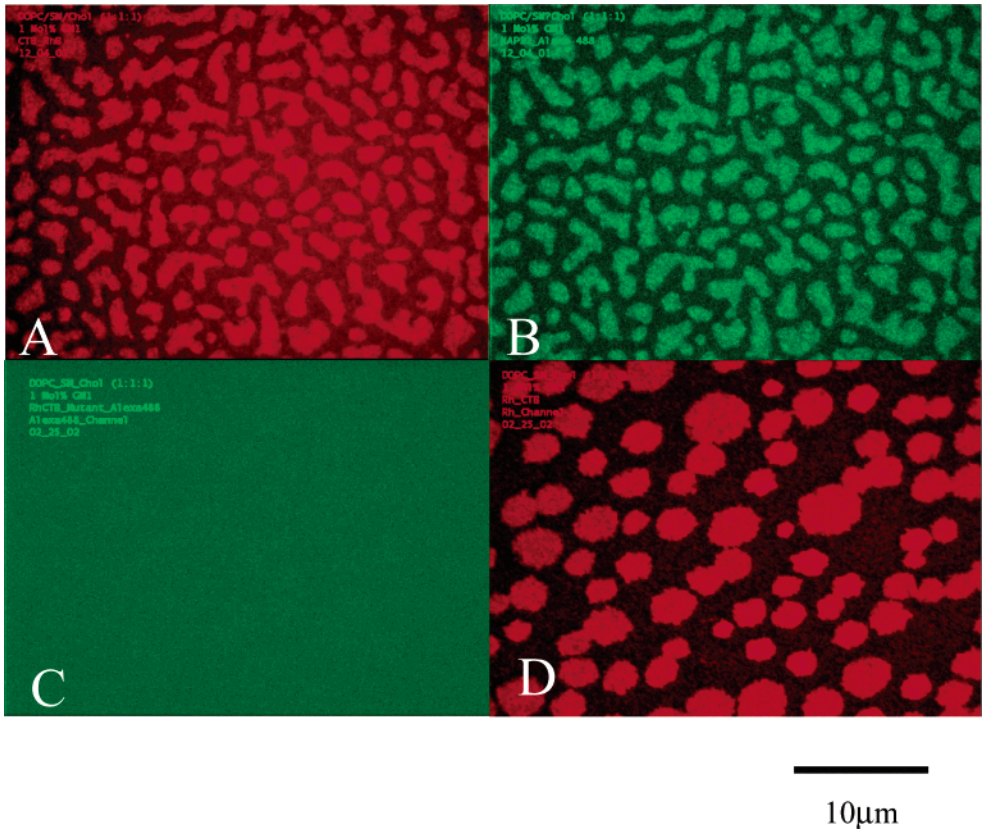

FIGURE 1: NAP-22 colocalizes with GM1-containing raft-like domains. Fluorescence micrographs show supported monolayers on silanized glass substrates formed from DOPC/Chol/SM (1:1:1) and 1 mol % GM1. (A) Raft-like domains containing GM1 were stained with Rh-CTxB. (B) The same domains were colabeled with Alex488-NAP-22. (C) Demyristoylated, Alexa488-labeled NAP-22 did not bind to raft-like domains in the specimen as visualized with Rh-CTxB (D). (C) and (D) are green and red channel images of identical regions.

fraction (*13*). NAP-22 also enriches the cholesterol content relative to phospholipid in the detergent-resistant fraction. Using fluorescence microscopy, we demonstrate in this report that NAP-22 binds raft-like domains in planar-supported monolayers in a manner that requires its myristoylation. NAP-22 binding protects raft-like domains against cholesterol extraction, and the binding is partially resistant to detergent extraction. When bound to raft-like domains, NAP-22 lateral mobility is extremely low. Exogeneously added NAP-22 binds to cell membranes and colocalizes to a degree with putative raft regions identified by cholera toxin staining of the glycospingolipids, GM1.

MATERIALS AND METHODS

Materials. 1,2-Dioleoyl-*sn*-glycero-3-phosphocholine (DOPC), cholesterol (Chol), brain sphingomyelin (SM), and ovine ganglioside GM1 (GM1) were purchased from Avanti Polar Lipids (Alabaster, AL). Lipid samples were dissolved in chloroform (HPLC grade) at a concentration of 1 mg/mL for the preparation of planar-supported lipid monolayers. The cholesterol sequestering agent methyl-β-cyclodextrin (MβCD), dimethyldichlorosilane, cholera toxin B subunit (CTxB), and cholera toxin B subunit conjugated with FITC (CTxB-FITC) were obtained from Sigma Chemical Co. (St. Louis, MO). NAP-22 was isolated from 2-week-old rat brains (*10*, *11*). Demyristoylated NAP-22 was expressed in *Escherichia coli* and purified as described (*14*). These proteins were conjugated to Alexa-488 (Alexa488-NAP-22) and Alexa-568 (Alexa568-NAP-22) with the kit supplied by Molecular Probes (Eugene, OR). Previous work has demonstrated that NAP-22 expressed in *E. coli* with *N*-myristoyl transferase is indistinguishable from myristoylated NAP-22 isolated from brain (*14*). Cholera toxin B subunit was labeled with lissamine rhodamine B sulfonyl chloride (Rh-CTxB) according to the procedure described by Molecular Probes.

Preparation of Planar-Supported Phospholipid Monolayers. The method used for the preparation of planar-supported phospholipid monolayers has been adapted from the literature (*6*, *15*, *16*). Briefly, argon ion plasma-cleaned glass cover slips were exposed to 0.5 mL of dimethyldichlorosilane placed in a desiccator. A partial vacuum was applied for 1 min. After 20 min the desiccator was filled with argon gas. The silanized glass cover slips were kept in a glass beaker and could be used for up to 5 days. Before use, cover slips were kept in a vacuum for 15 min. Seventy microliters of a solution in chloroform containing a mixture of DOPC, SM, and Chol (total lipid concentration =2.3 mM, 1:1:1 molar ratio) and 1.0 mol % GM1 was spread on the air−water interface of a Langmuir trough at room temperature. The monolayers were slowly compressed to 32 dyn/cm and then transferred to silanized cover slips at room temperature. Cover slips containing deposited monolayers were mounted on glass slides with spacers to form chambers with ~80 μL volume, and at room temperature, the supported monolayers were washed five times with 100 μL of HB (20 mM Hepes, pH 7.3). Monolayers were then treated with 80 μL of Alexa488-NAP-22 (10 μg/mL in HB) and/or 100 μL of Rh-CtxB (2.5 μg/mL in HB) for 5 min. Free protein was removed by washing five times with 100 μL of HB. For nonionic detergent extraction experiments, TNE (25 mM Tris-

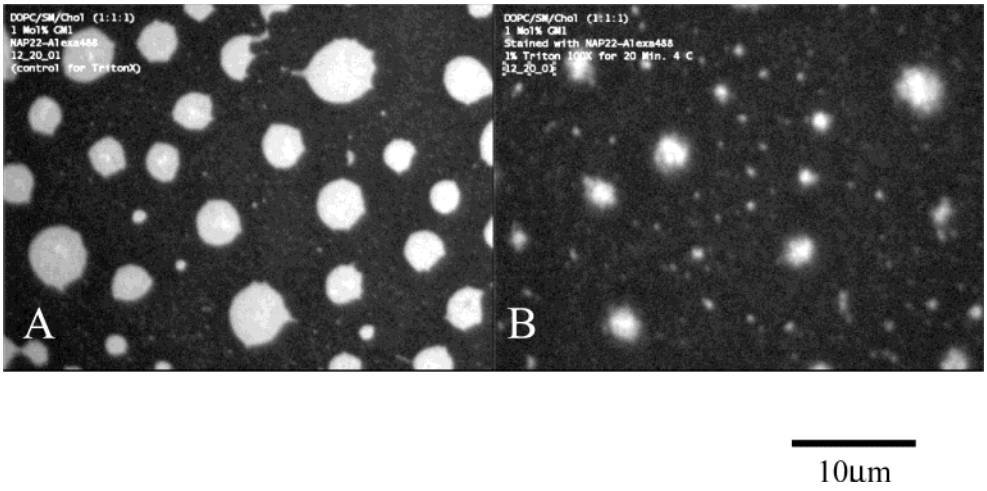

FIGURE 2: Binding of NAP-22 to raft-like domains is partially resistant to detergent extraction. Fluorescence micrographs show supported monolayers on silanized glass substrates formed from DOPC/Chol/SM (1:1:1) and 1 mol % GM1. (A) Raft-like domains are visualized by Alexa-NAP-22 binding. (B) Significant remnants of such domains remain following nonionic detergent extraction at 4 °C.

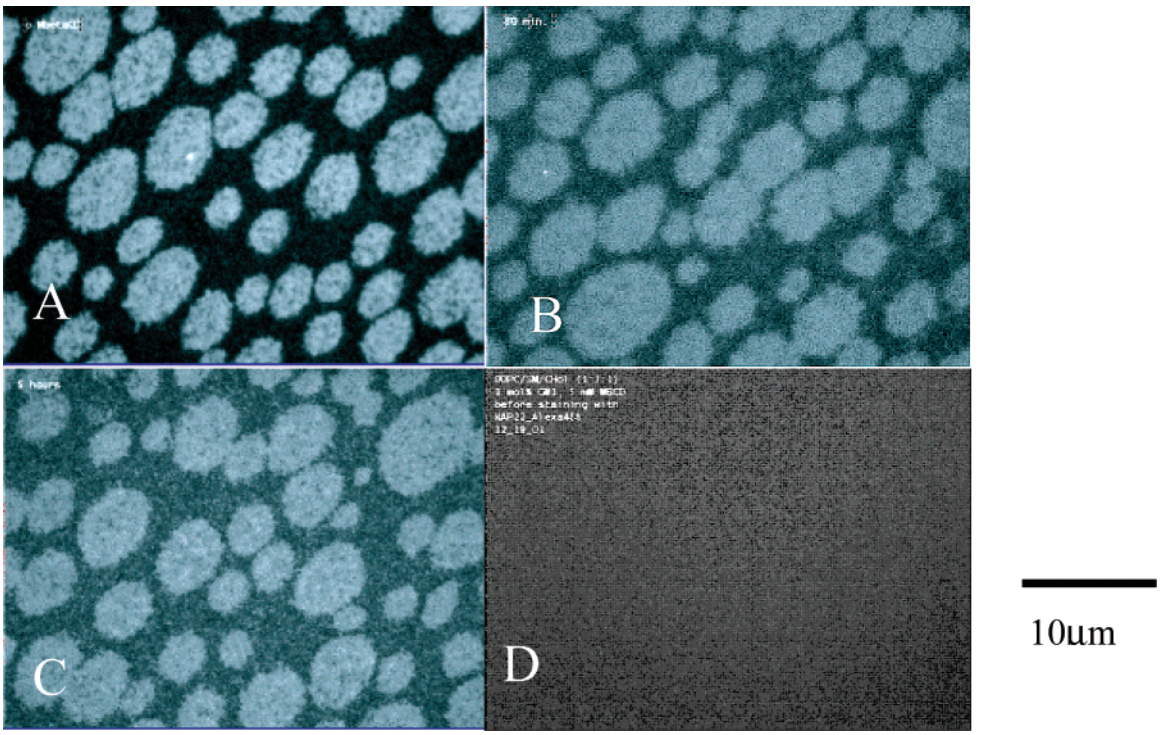

FIGURE 3: NAP-22 protects raft-like domains from cholesterol extraction. Fluorescence micrographs show supported monolayers on silanized glass substrates formed from DOPC/Chol/SM (1:1:1) and 1 mol % GM1. (A) Cholesterol-rich raft-like domains are stained with Alexa488-NAP-22. (B, C) The domains remain after extraction with 5 mM MβCD for 30 min (B) or 10 mM MβCD for 5 h (C). (D) Preextraction of cholesterol with 10 mM MβCD for 30 min prevents staining by Alexa-NAP-22.

HCl, 150 mM NaCl, 5 mM EDTA, pH 7.5) containing 1% Triton X-100 buffer was used. TNE is a buffer generally used for making detergent-resistant membrane preparations. First, monolayers pretreated with Alexa-NAP-22 were washed three times with 100 μL of TNE buffer, and then 100 μL of the same TNE buffer containing 1% Triton X-100 was added to the chamber containing the supported monolayer at 4 °C and kept for 20 min. After detergent treatment the supported monolayer was washed five times with 100 μL of HB to remove the detergent-soluble materials. For cholesterol extraction studies, monolayers were treated with MβCD in HB at specified concentrations (5, 10, 50 mM) and for specified times (30 min, 5 h) and then washed five times with 100 μL of HB.

Cell Culture and Labeling. 3T3L1 fibroblast cells, a continuous substrain of Swiss albino (American Type Culture Collection, Rockville, MD), were maintained in Dulbecco's modified Eagle's medium (DMEM) (Sigma Chemical Co., St. Louis, MO) that had been supplemented with 10% fetal bovine serum, 100 units/mL penicillin, and 100 μg/mL streptomycin. C3H10T1/2 murine fibroblast cells (American Type Culture Collection, Rockville, MD) were maintained in basal Eagle medium with Earle's salts and L-glutamine (BME) that had been supplemented with 10% fetal bovine serum, 100 units/mL penicillin, and 100 μg/mL streptomycin. Cells were plated on 22 × 22 mm 1.5 glass cover slips (Fisher Scientific, Pittsburgh, PA) that had been placed in 35 mm tissue culture dishes. After 2−4 days, 60−70% confluent cells were used

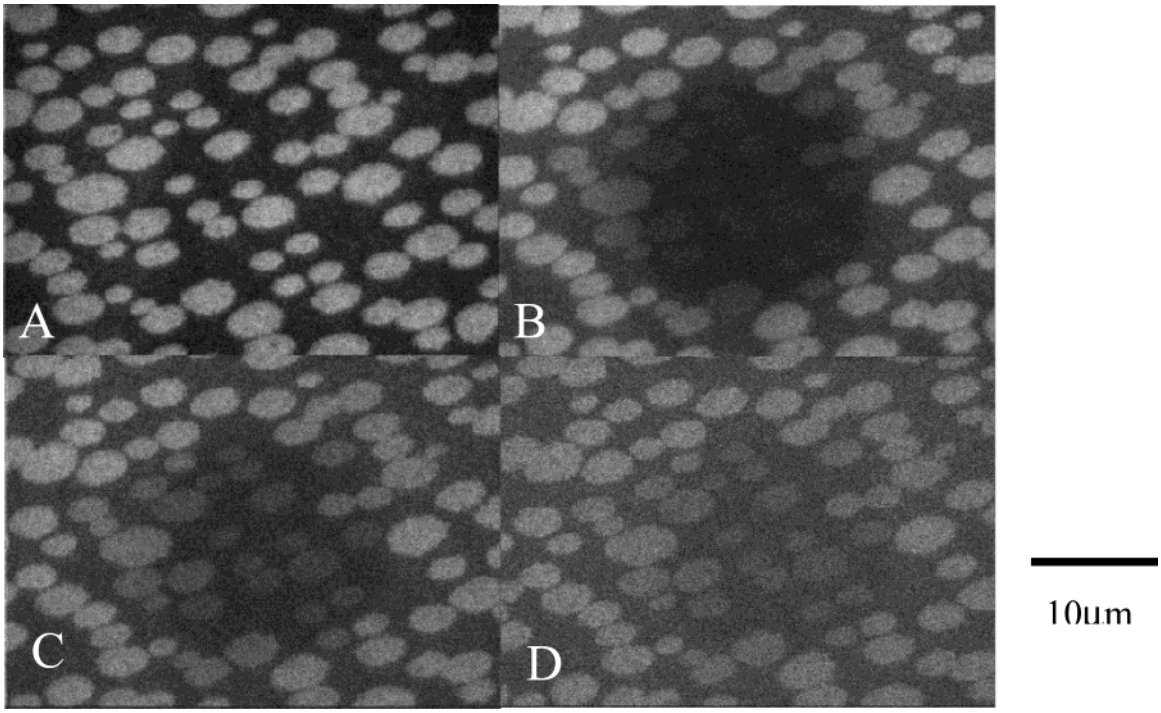

FIGURE 4: Alexa-NAP-22 bound to raft-like domains exhibits low lateral mobility. Fluorescence micrographs show supported monolayers on silanized glass substrates formed from DOPC/Chol/SM (1:1:1) and 1 mol % GM1 before and after a large area photobleaching. (A) Cholesterol-rich domains are stained with Alexa-NAP-22. Subsequent images were taken (B) immediately after photobleaching, (C) 30 min after photobleaching, and (D) 60 min after photobleaching.

for fluorescence microscopy. After being washed three times with PBS+ (Dulbecco's phosphate-buffered saline with calcium chloride and magnesium chloride), cells were labeled with 150 μL of Alexa488-NAP-22 (10 μg/mL in PBS+) for 5 or 10 min at room temperature and washed three times with PBS+. When required, the cells were subsequently labeled with 150 μL of CTxB-Rh (10 μg/mL in PBS+) for 5 or 10 min and washed three times with PBS+.

Wide-Field and Laser Scanning Fluorescence Microscopy. Fluorescence micrographs of the supported monolayers and cells were made with an inverted microscope (Axiovert 10 with 100×/1.30 Plan-NeoFluar; Zeiss, Holmdale, NJ) equipped with a CCD camera (Micromax, 782 × 582 chip; Princeton Instruments, Trenton, NJ). All of the images shown are digitized to 12 bits with 0.08 μm pixel resolution and were taken at room temperature. Two-color images were produced using fluorescein and rhodamine channels.

For confocal microscopy, cells were mounted and imaged using a Zeiss 510 laser scanning confocal microscope (Carl Zeiss, Thornwood, NY). Excitation was at 488 nm, and a 100× PlanApochromat objective was employed in conjunction with a 153 μm pinhole (effective optical section depth approximately 0.8 μm).

Imaging of Detergent-Resistant Membrane in Cells. Two-day-old 70−80% confluent C3H10T1/2 cells were washed three times with PBS+ followed by a treatment with TNE (25 mM Tris-HCl, pH 7.5, 150 mM NaCl, 5 mM EDTA) buffer containing 1% Triton X-100 for 20 min at 4 °C. After being washed three times with PBS+, cells were labeled with Alexa488-NAP-22 for 5 min at room temperature and washed three times with PBS+. Next, the cells were labeled with CTxB-Rh for 5 min and washed three times with PBS+. Detergent-treated cells were imaged in FITC and rhodamine channels using an inverted microscope (Zeiss Axiovert 10 with 100×/1.30 Plan-NeoFluar objective; Zeiss, Holmdale, NJ).

Relative Partitioning of Probes between Raft-like and Liquid-Disordered Domains. The relative partitioning between raft-like and liquid-disordered domains in monolayers was quantified as described elsewhere (*17*). Briefly, the average intensities of different domains were measured from the images recorded on the CCD. The relative partition coefficient is defined as $R = I_R/(I_R + I_N)$, where I_R and I_N are the background-corrected average intensities of raft and nonraft domains. The average *R*-values were calculated from at least four different measurements.

Detergent-Resistant Membrane (DRM) Fractionation Using a Sucrose Gradient. DRM fractionation was done using standard methods (*18*). Briefly, 100% confluent 3T3L1 cells in 10 cm tissue culture dishes were washed three times with PBS+ at room temperature and incubated for 10 min with 2 mL of PBS+ containing 20 μL of Alexa568-NAP-22 (1 mg/mL). After being washed three times with PBS+, cells were again incubated for 10 min with 2 mL of PBS+ containing 20 μL of CTxB-FITC (1 mg/mL) and washed three times with PBS+. Cells were then lysed at 4 °C using TNE buffer containing 1% Triton X-100 for 20 min and then were scraped from the dishes with a rubber policeman and homogenized. The lysate was adjusted to 40% sucrose in TNE buffer with 1% Triton X-100 using 80% sucrose in TNE containing 1% Triton X-100 (total volume 2.5 mL); it was placed in an ultracentrifuge tube overlaid with 2 mL of 38% sucrose in TNE with 1% Triton X-100 followed by 0.5 mL of 5% sucrose in buffer with 1% Triton X-100 and centrifuged for 20 h at 36000 rpm using an SW55Ti rotor in a Beckman L7 ultracentrifuge. Triton X-100 insoluble membranes were at the interface between the 5% and 38% sucrose layers. The sucrose gradient column was divided into

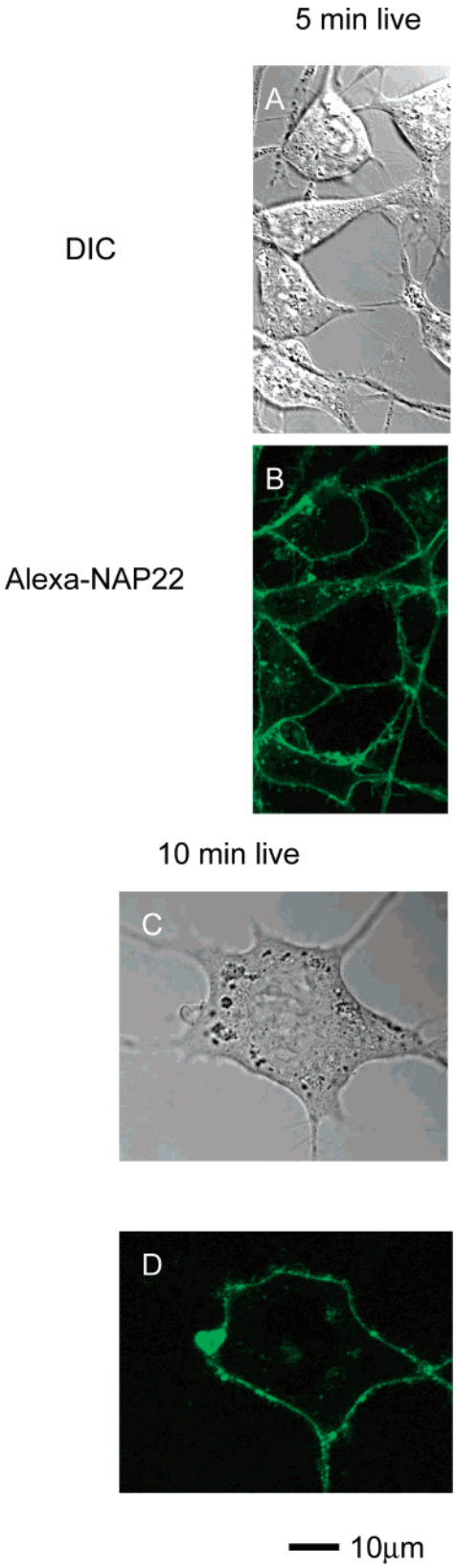

FIGURE 5: Staining of Alexa-NAP-22 on 3T3L1 cells. Laser scanning confocal images of Alexa488-NAP-22-stained live 3T3L1 fibroblast cells. (A) Laser scanning confocal DIC image of live 3T3L1 cells after 5 min incubation with Alexa-NAP-22; (B) corresponding laser scanning confocal fluorescence image; (C, D) corresponding images after 10 min incubation with Alexa488-NAP-22. Optical sections are near the substrate.

10 fractions. The fluorescence intensity of each fraction was measured in a Simadju spectrofluorometer. For Alexa568-NAP-22 each fraction was 200 times diluted to reduce the light scattering; emission and excitation filters were set to 640 and 568 nm, respectively. For CTxB-FITC, each fraction was 20 times diluted to reduce the light scattering during fluorescence intensity measurement; emission and excitation filters were set to 510 and 488 nm, respectively.

RESULTS AND DISCUSSION

Colocalization of NAP-22 with GM1 in Raft-like Domains in Planar-Supported Monolayers. NAP-22 binding to model membranes containing cholesterol has been reported for sonicated vesicles (*11*) and for multilamellar vesicles (*13*). Planar-supported monolayers formed from the lipid mixture (DOPC/Chol/SM, 1:1:1) and 1.0 mol % GM1 show clear domain formation after labeling with Rh-CTxB (Figure 1A), as reported earlier (*6*, *17*). Such domains were also visible by labeling with Alexa488-NAP-22, suggesting that these domains are cholesterol-rich (Figure 1B). Demyristoylated NAP-22 does not bind significantly to DOPC/Chol/SM monolayers (Figure 1C) even though they contain raft-like domains as visualized with Rh-CTxB (Figure 1D). The relative partitioning of NAP-22 between the raft-like and nonraft phase has been calculated from the fluorescence micrographs, confirming the high affinity of this protein for cholesterol-rich domains. The relative partition coefficients, R, of GM1 and NAP-22, when both components are present, are 0.66 ± 0.04 and 0.59 ± 0.02, respectively. (The R-value for GM1 alone exceeds 0.8.) Thus, these R-values are similar to what was previously measured for Thy-1 ($R \approx 0.6$), a GPI-anchored protein (*17*).[2] Our results suggest that NAP-22 binds cholesterol-rich domains and that such binding requires the myristoyl chain. Indeed, the membrane binding energy of NAP-22 to liposomes containing cholesterol is very similar to the binding energy of myristate to membranes (*13*, *19*). This result suggests that the protein moiety of NAP-22, containing a considerable amount of β-structure, has low intrinsic affinity for the membrane as is experimentally confirmed (*13*).

NAP-22 Binding to Raft-like Domains Is Partially Resistant to Detergent Extraction. Raft-like lipid domains are resistant to nonionic detergents (*6*). Planar-supported monolayers made from DOPC/SM/Chol (1:1:1) containing 1 mol % GM1 were labeled with Alexa488-NAP-22 (Figure 2A). Following extraction with TNE for 20 min at 4 °C, detergent-resistant raft-like domains were still visible in the Alexa-488 channel (Figure 2B) although the shapes of the domains were changed. Thus, NAP-22 binding to raft-like domains can withstand the rigors of detergent extraction to a significant extent. This result corroborates the finding that NAP-22 is found in detergent-resistant fractions following detergent extraction of NAP-22 bound to cholesterol-rich vesicles (*11*, *13*) and is consistent with the fact that NAP-22 is found in detergent-resistant membrane preparations from neuronal tissue (*11*).

NAP-22 Appears To Stabilize Cholesterol-Rich Raft-like Domains. Methyl-β-cyclodextrin is a cholesterol sequestering reagent generally used to extract cholesterol from model as well as cell membranes. This reagent has the ability to disrupt raft-like domains by extracting cholesterol, and this phen-

[2] It is possible that R will depend on the total density of the molecule of interest. Furthermore, different molecules may compete for occupancy in raft-like domains, altering the measured partitioning (*17*).

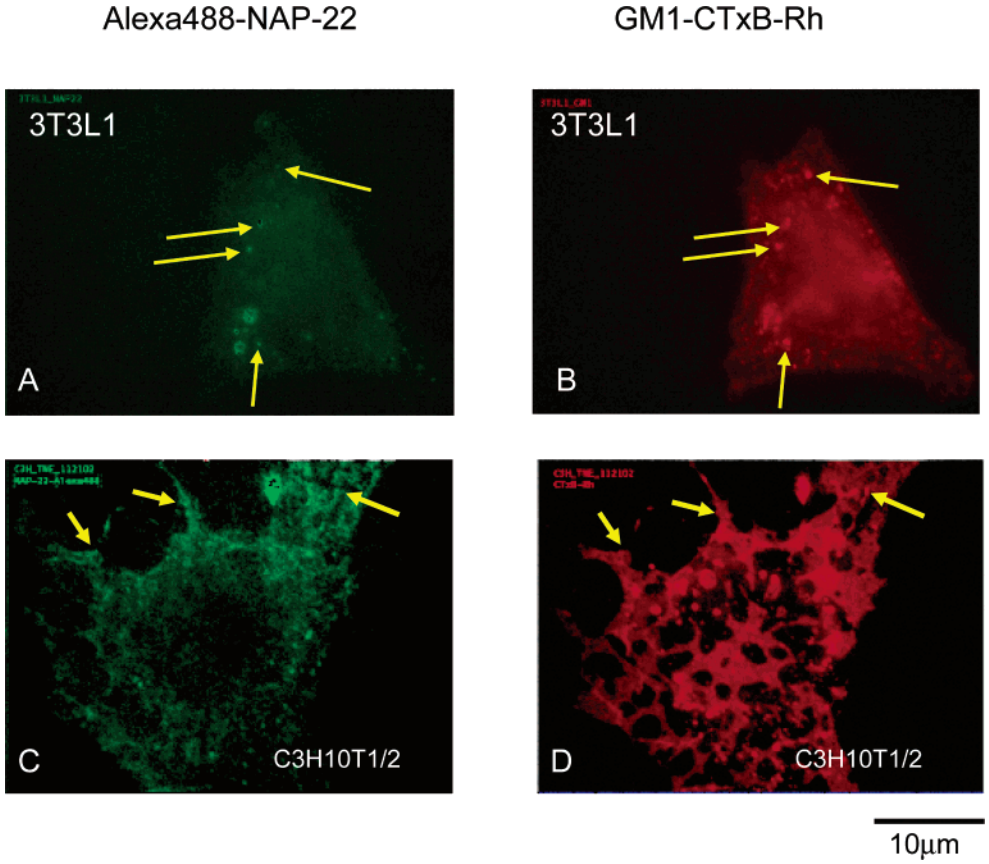

FIGURE 6: Colocalization of NAP-22 and GM1 in live and detergent-extracted cells. (A, B) Wide-field micrographs were taken after colabeling live cells with Alexa488-NAP-22 (A) and CTxB-Rh (B). (C, D) Fluorescence microscopic images of TNE (25 mM Tris-HCl, 150 mM NaCl, 5 mM EDTA, pH 7.5, containing 1% Triton X-100) buffer treated cells colabeled with Alexa488-NAP-22 (C) and CTxB-Rh (D). In both (A, B) and (C, D), arrows show regions of stain colocalization.

omenon has also been observed in model membranes (*17*, *20*). Cholesterol-rich raft-like domains are stained with Alexa-NAP-22 (Figure 3A). When monolayers containing raft-like domains labeled with Alexa488-NAP-22 are treated with 5 mM MβCD for 30 min (Figure 3B) or 10 mM MβCD for 5 h (Figure 3C), the domains are not appreciably disrupted by this treatment. This observation strongly suggests that NAP-22 binding stabilizes such domains against cholesterol extraction, although it is theoretically possible that NAP-22 remains on the membrane after cholesterol has been removed. Calculations of the relative partition coefficient of NAP-22 after cholesterol extraction at different doses of MβCD treatment indicate that the affinity toward the cholesterol-containing raft-like domains is not changed by MβCD treatment. NAP-22 does not label raft monolayers previously extracted by MβCD (Figure 3D). Cholesterol can be extracted by a higher dose of MβCD (50 mM) in the presence of NAP-22 (results not shown).

The Lateral Mobility of NAP-22 Bound to Raft-like Domains Is Very Low. Figure 4A shows a fluorescence image of a DOPC/Chol/SM (1:1:1) monolayer labeled with Alexa-NAP-22. A selected area of the specimen (radius 8.33 μm) was photobleached with 488 nm light from a mercury lamp on a microscopic stage (Figure 4B), and recoveries were imaged after 30 min (Figure 4C) and 60 min (Figure 4D). These measurements indicated, qualitatively, that the lateral mobility of the bound Alexa-NAP-22 was very low. Roughly speaking, these measurements yield a diffusion coefficient, D, of $\sim$0.006 $\mu m^2/s$, based on the estimated recovery time and spot radius. This approximate diffusion coefficient was much lower than that of fluorescein-conjugated DPPE in monolayers made from DOPC/Chol/SM ($D = 0.33$ $\mu m^2/s$) and of DPPE conjugated with Texas Red in monolayers formed from a lipid extract from the brush border membranes of rat kidney cells ($D = 0.46$ $\mu m^2/s$) (*17*). This result indicates that NAP-22 has an extremely low mobility, possibly because it forms two-dimensional pseudocrystals when bound to cholesterol-rich domains (*13*). The very low lateral mobility of NAP-22, its resistance to detergent extraction, and its protection of raft-like domains to cholesterol extraction all suggest a tight organization of NAP-22 on the surface of cholesterol-containing raft-like domains.

Biological Implications. This study suggests that NAP-22 binding may be employed to image cholesterol-rich regions, such as caveolae/rafts on the plasma membrane of cells. Indeed, immunofluorescence of expressed NAP-22 demonstrated colocalization of NAP-22 and cholesterol in the plasma membrane and the Golgi at relatively low resolution (*14*). In Figure 5, Alexa488-NAP-22 was added externally to Swiss 3T3L1 fibroblasts and imaged in a laser scanning confocal microscope focused close to the ventral surface membrane. The image is heterogeneous with some NAP-22 remaining relatively uniform and other NAP-22 residing in puncta, perhaps representing clustured caveolae/rafts. In Figure 6A,B, Alexa488-NAP-22 and rhodamine CTxB (to image GM1) were employed to simultaneously label NAP-22 and GM1 in 3T3L1 fibroblasts and imaged in a wide-field microscope. In these wide-field images, some

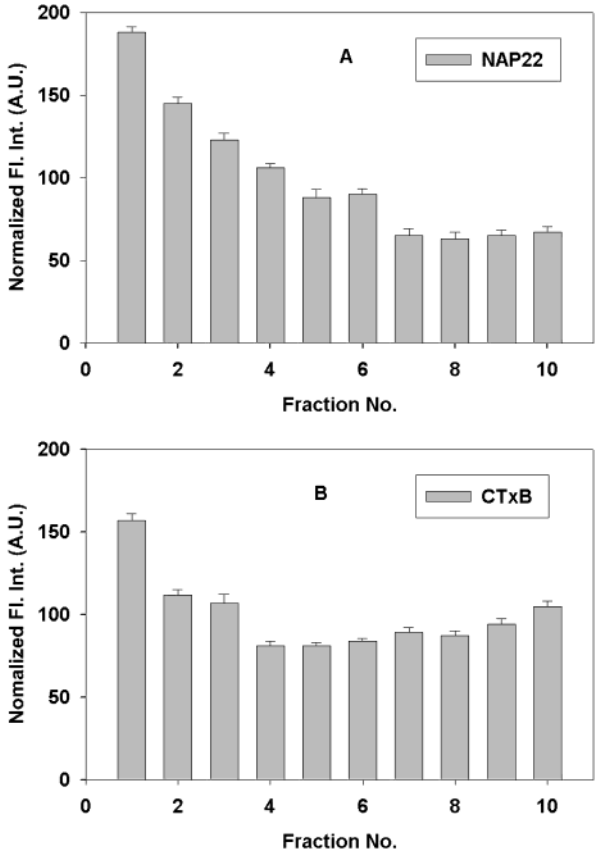

FIGURE 7: Extent of cofractionation of NAP-22 and GM1 (labeled with CTxB-FITC) in detergent-resistant membrane preparations. Normalized fluorescence intensity (Fl Int) in arbitrary units (AU) of Alexa568-NAP-22 (A) and CTxB-FITC (B) for 10 different fractions from a sucrose gradient column. (Fraction 1 is at the top of the gradient and corresponds to the 5−38% sucrose interface.) The error bars indicate the standard error for four separate preparations.

NAP-22 colocalizes with GM1 (arrows in panels A and B), but clearly there is not perfect coincidence. It appears that the higher lateral resolution afforded by immunoelectron microscopy will be required to assess the degree of colocalization more precisely (*21*−*23*). We also performed a colocalization study in detergent-extracted cells (Figure 6C,D), which again shows partial (arrows in panels C and D) but not complete colocalization. In general, NAP-22 staining appears as an imperfect subfraction of GM1 staining. Consistent with this, raft isolation on a sucrose gradient (Figure 7) shows a substantial amount of both GM1 and NAP 22 floating in the low-density fractions, but in 3T3L1 cells, some of both materials appears all across the gradient.

NAP-22 is found on the cytoplasmic face of the plasma membrane of neuronal cells where it may to bind to preexisting cholesterol-rich domains. In this role, the potential of NAP-22 to compete with other signal transduction partners for sites on the inner monolayer raft may cause it to inhibit raft-dependent signal transduction. Alternatively, NAP-22 may be involved in organizing cholesterol-rich domains in the inner monolayer perhaps, in this way, promoting transbilayer communication required for functions such as signal transduction. As a cell biological tool, the binding of externally added NAP-22 to caveolae/rafts may potentially be employed to modulate their respective functions.

REFERENCES

1. Jacobson, K., and Dietrich, C. (1999) Looking at lipid rafts?, *Trends Cell Biol. 9*, 87−91.
2. Simon, K., and Ikonen, E. (1997) Functional rafts in cell membranes, *Nature 387*, 569−572.
3. Simons, K., and Toomre, D. (2000) Lipid rafts and signal transduction, *Nat. Rev. Mol. Cell Biol. 1*, 31−39.
4. Anderson, R. G. W., and Jacobson, K. (2002) A Role for Lipid Shells in Targeting Proteins to Caveolae, Rafts, and Other Lipid Domains, *Science 296*, 1821−1825.
5. Brown, D. A., and London, E. (1998) Functions of lipid rafts in biological membranes, *Annu. Rev. Cell Dev. Biol. 14*, 111−136.
6. Dietrich, C., Bagatolli, L. A., Volovyk, Z. N., Thompson, N. L., Levi, M., Jacobson, K., and Gratton, E. (2001) Lipid Rafts Reconstituted in Model Membranes, *Biophys. J. 80*, 1417−1428.
7. Edidin, M. (2001) Shrinking patches and slippery rafts: scales of domains in the plasma membrane, *Trends Cell Biol. 11*, 492−496.
8. Hao, M., Mukherjee, S., and Maxfield, F. R. (2001) Cholesterol depletion induces large scale domain segregation in living cell membranes, *Proc. Natl. Acad. Sci. U.S.A. 98*, 13072−13077.
9. Waheed, A. A., Shiada, Y., Heijnen, H. F. G., Nakamura, M., Inomata, M., Hayashi, M., Iwsahita, S., Slot, J. W., and Ohno-Iwashita, Y. (2001) Selective binding of perfringolysin O derivative to cholesterol-rich membrane microdomains (rafts), *Proc. Natl. Acad. Sci. U.S.A. 98*, 4926−4931.
10. Maekawa, S., Maekawa, M., Hattori, S., and Nakamura, S. (1993) Purification and molecular cloning of a novel acidic calmodulin binding protein from rat brain, *J. Biol. Chem. 268*, 13703−13709.
11. Maekawa, S., Sato, C., Kitajima, K., Funatsu, N., Kumanogoh, H., and Sokawa, Y. (1999) Cholesterol-dependent Localization of NAP-22 on a Neuronal Membrane Microdomain (Raft), *J. Biol. Chem. 274*, 21369−21374.
12. Iino, S., Kobayashi, S., and Maekawa, S. (1999) Immunohistochemical localization of a novel acidic calmodulin-binding protein, NAP-22, in the rat brain, *Neuroscience 91*, 1435−1444.
13. Epand, R M., Maekawa, S., Yip, C. M., and Epand, R. F. (2001) Protein-Induced Formation of Cholesterol-Rich Domains, *Biochemistry 40*, 10514−10521.
14. Terashita, A., Funatsu, N., Umeda, M., Shimada, Y., Ohno-Iwashita, Y., Epand, R. M., and Shohei Maekawa, S. (2002) The lipid binding activity of a neuron specific protein NAP-22 studied *in vivo* and *in vitro*, *J. Neurosci. Res. 70*, 172−179.
15. Merkel, R., Sackmann, E., and Evans, E. (1989) Molecular friction and epitactic coupling between monolayers in supported bilayers, *J. Phys. (France) 50*, 1535−1555.
16. Tscharner, V., and McConnell, H. M. (1981) Physical properties of lipid monolayers on alkylated planar glass surfaces, *Biophys. J. 36*, 421−427.
17. Dietrich, C., Volovyk, Z. N., Levi, M., Thompson, N. L., and Jacobson, K. (2001) Partitioning of Thy-1, GM1, and cross-linked phospholipid analogues into lipid rafts reconstituted in supported model membrane monolayers, *Proc. Natl. Acad. Sci. U.S.A. 98*, 10642−10647.
18. Arreaza, G., Melkonian, K. A., LaFevre-Bernt, M., and Brown, D. A. (1994) Triton X-100-resistant membrane complexes from cultured kidney epithelial cells contain the Src family protein tyrosine kinase p62yes, *J. Biol. Chem. 269*, 19123−19127.
19. Peitzsch, R. M., and McLaughlin, S. (1993) Binding of acylated peptides and fatty acids to phospholipid vesicles: Pertinence to myristoylated proteins, *Biochemistry 32*, 10436−10443.
20. Radhakrishnan, A., and McConnell, H. M. (2000) Chemical Activity of Cholesterol in Membranes, *Biochemistry 39*, 8119−8124.
21. Prior, I. A., Muncke, C., Parton, R. G., and Hancock, J. F. (2003). Direct visualization of Ras proteins in spatially distinct cell surface microdomains, *J. Cell Biol. 160*, 165−170.
22. Madore, N., Smith, K. L., Graham, C. H., Jen, A., Brady, K., Hall, S., and Morris, R. (1999) Functionally different GPI proteins are organized in different domains on the neuronal surface, *EMBO J. 18*, 6917−6926.
23. Wilson, B., Pfeiffer, J., and Oliver, J. (2000) Observing FcϵRI signalling from the inside of the mast cell membrane, *J. Cell Biol. 149*, 1131−1142.

BI0265877